IEEE/CSC & ESAS SUPERCONDUCTIVITY NEWS FORUM (global edition), January 2016.
EUCAS 2015 invited presentation 3M-E-O1.6. Submitted to IEEE Trans. Appl. Supercond. for possible publication.

Simulation of HTS Josephson mixers

Colin Pegrum, Ting Zhang, Jia Du and Yingjie Jay Guo

***Abstract*—CSIRO has developed superconducting Microwave Monolithic Integrated Circuit (MMIC) mixers using step-edge Josephson junctions and on-chip filters, made from YBaCuO on MgO substrates. Integration into a MMIC results in a compact and efficiently-coupled structure. These have been shown to have outstanding conversion efficiency, dynamic range and linearity.**

We report here a range of simulations of this type of mixer. We have mainly used Josephson simulators and analyse the data in both the time and frequency domains. More recently we also use microwave simulators incorporating a novel Verilog-A Josephson junction model that we have developed. We have looked at the interactions of junction bias current, local oscillator power and RF input power with conversion efficiency, dynamic range and linearity. Good agreement is found overall with measurements.

***Index Terms*—MMIC, Superconducting microwave devices, Josephson mixers, heterodyning.**

I. Introduction

CSIRO has recently demonstrated a range of single-junction externally-pumped mixers, which use an HTS step-edge junction [1], [2], a radio-frequency (RF) input bandpass filter (BPF), a low-pass filter (LPF) at the output intermediate frequency (IF) and a transmission-line resonator for the local oscillator (LO) input (which stops RF leakage back into the LO port). All components are integrated as a Monolithic Microwave Integrated Circuit (MMIC) on a single MgO substrate. This results in a compact and efficiently-coupled structure. Details about the CSIRO HTS step-edge junction technology can be found in [1] and [2]. The filter design and performance is described in [3]–[5].

First-generation devices operated typically at 7 to 12 GHz [6]–[8] and recently a 30 to 33 GHz Ka device been reported [9]. Fig. 1 shows a packaged MMIC with a $10-12$ GHz BPF, a 4 GHz cut-off LPF and an 8 GHz LO filter [6]. The simulation results reported here relate to this device.

II. Modelling approaches

We model the MMIC mixer in two different ways. The first uses Agilent's Advanced Design System (ADS) [10], a powerful microwave design and simulation package. The second is based on the well-tried and freely-available Josephson simulator JSIM [11], [12] with various custom post-processing routines.

Manuscript received 8 September 2015. Colin Pegrum is with the Department of Physics, University of Strathclyde, Glasgow G4 0NG, UK (e-mail: colin.pegrum@strath.ac.uk).

Ting Zhang is with CSIRO, Lindfield, NSW 2070, Australia (e-mail: ting.zhang@csiro.au).

Jia Du is with CSIRO, Lindfield, NSW 2070, Australia (e-mail: jia.du@csiro.au).

Yingjie Jay Guo is with the University of Technology, Sydney, Australia (e-mail: jay.guo@uts.edu.au).

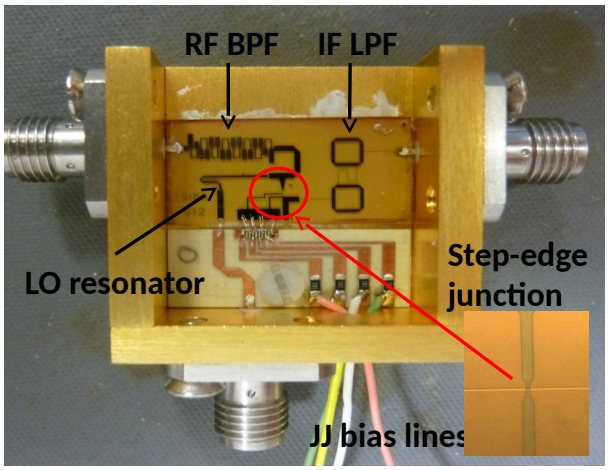

Fig. 1. Photo of a packaged HTS MMIC, with $10-12$ GHz input and 8 GHz LO, taken from [6]. The MgO substrate is $10\,\text{mm} \times 20\,\text{mm}$. The inset shows the $2\,\mu$m wide step-edge junction.

A. Agilent Advanced Design System (ADS)

ADS can simulate accurate models of the various microwave filters in the MMIC. But as supplied it has no built-in model for a Josephson junction, so we have adapted a Verilog-A model from [13] and imported this into ADS. Preliminary results have been reported recently elsewhere [14] and agree well with experimental measurements. The Verilog-A model has also been separately tested using the Qucs simulator [15] and a Josephson junction, just with DC bias: its time-domain results agree precisely with those from JSIM. (Qucs also has a wide range of microstrip components, and filter design packages, but these are only supported in the frequency domain in its present version, so Qucs cannot be used currently for our time-domain simulations.)

This paper reports work using the JSIM approach.

B. JSIM

JSIM has only a simple transmission line model, so it is not possible to use it to represent the complex microstrip filters used in the MMIC. Initially we designed instead $50\,\Omega$ band-pass and low-pass filters using discrete inductors, capacitors and resistors. But there are two serious issues with this approach: the out-of-band impedances of these filters are very different to those of the real microstrip filters, so the broadband behaviour will not be representative; also, the large number of components needed to get high-order filters causes JSIM to run unacceptably slowly.

So instead we simplified the model to the minimum possible, as in Fig. 2. This uses AC current sources for the RF and LO inputs. Current sources have infinite impedance, so

they provide perfect mutual isolation. We expect this simplified model to show the maximum conversion efficiency possible: it has no filter losses, and there are no mismatch issues between the filters and the low-resistance junction.

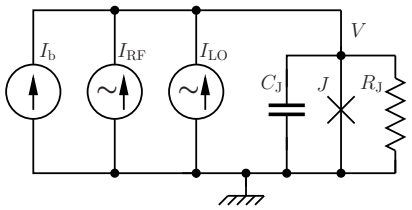

Fig. 2. Our simplified JSIM mixer model. The junction has a DC current source for bias I_b. AC current sources I_{RF} and I_{LO} provide RF and LO inputs.

For all of the simulations reported here, the critical current $I_c = 774\,\mu$A, the junction resistance $R_J = 2.5\,\Omega$, its $C_J = 18$ fF [16], and the simulation temperature $T = 40$ K in most cases. The RF, LO and IF frequencies f_{RF}, f_{LO} and f_{IF} are 10.4, 8 and 2.4 GHz respectively. All these parameters match those of the experimental device [6], so we can compare simulation and experiment. In addition, we have modelled mixers with quite different junction characteristics, e.g. $I_c = 100\,\mu$A, $R_J = 20\,\Omega$, which match the experimental results in [7]. Those results (none are shown here) are qualitatively the same. Note that the latter junction is hysteretic with no RF or LO drive, but with LO turned on, the hysteresis is suppressed.

III. Outline of the Simulation Procedure

JSIM time-domain data for the mixer output voltage $V(t)$ was generated by parallel processing on a 4 or 8 core CPU. The power spectral density (PSD) of $V(t)$ was got by an Octave or Matlab post-processing script using the `pwelch` function, with sampling rates and durations set for adequate frequency and amplitude resolution. A typical mixer PSD at $T = 40$ K is shown in Fig. 3. The script locates spectral peaks around the RF, LO and IF frequencies in the PSD, using the built-in `findpeaks` function, with an adaptive amplitude threshold detector, and measures their powers P_{RF}, P_{LO} and P_{IF} and the conversion efficiency $\eta = P_{IF}/P_{RF}$. The dynamic resistance $R_d = V_{RF}/I_{RF}$ is also estimated from the voltage amplitude V_{RF} of the RF signal from the PSD. The correct normalisation factors are applied [17] for the Hanning window used, and the amplitude and power calibration was confirmed by a test circuit with the junction replaced by just a resistor.

IV. Critical Current Suppression

We looked first at current-voltage (I-V) characteristics and the dependence of $I_c(I_{LO})$ on the LO amplitude I_{LO}, with no RF input, Figs. 4(a) and (b). We found the I_c suppression varies very linearly with LO amplitude:

$$I_c(I_{LO}) = I_c(0) - I_{LO} \qquad (1)$$

as shown in Fig. 4(b). This linearity is also seen in our experimental measurements, Figs. 5(a) and (b), for this single-junction mixer [6]. We saw this previously [18]. We find also that $I_c(I_{LO})$ remains fully suppressed for $I_{LO} > I_c(0)$, both

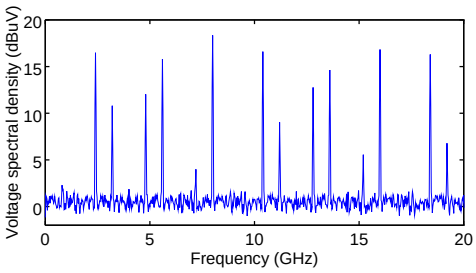

Fig. 3. A typical spectrum, for $f_{RF} = 10.4$ GHz and $f_{LO} = 8$ GHz. Mixing of harmonics of f_{RF} and f_{LO} generates the extra peaks in addition to $f_{IF} = 2.4$ GHz.

in simulation and experiment. This departure from the Bessel-like response expected for a voltage-driven junction is because the junction is current-driven, and also because the Josephson frequency $f_J \approx 900\,\text{GHz} >> f_{LO}$ [19].

From Figs. 4(b) and 5(a) we can relate the experimental LO power to the LO current amplitude in the simulation; e.g. an LO power of -40 dB is equivalent to a LO amplitude of 302μA.

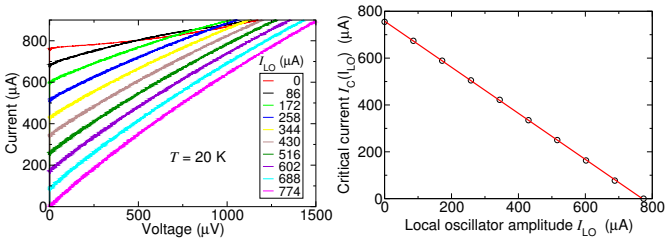

(a) (b)

Fig. 4. Simulation data, (a) a set of I-V curves for increasing I_{LO}; (b) The critical current suppression is a linear function of I_{LO}.

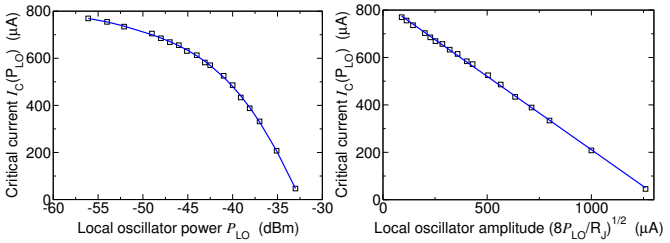

(a) (b)

Fig. 5. Experimental data at $T = 40$ K for the critical current (a) as a function LO power (b) showing its linear dependence on the LO voltage. Data from [6].

V. Effects of Noise

Most experimental measurements were done at $T = 40$ K. At this temperature the junction noise-rounding parameter $\Gamma(I_c) = (2\pi k_B T)/(I_c \Phi_0) \approx 2 \times 10^{-3}$ for $I_c = 774\,\mu$A and therefore thermal noise has little effect on the I-V characteristics in the absence of RF or LO input.

In simulations at $T = 0$ K, with LO input at 8 GHz at typical levels, microwave-induced steps can be seen, as in Fig. 6. Their step height $\Delta I_c \approx 10\,\mu$A and since $\Gamma(10\,\mu\text{A}) = 0.17$ at 40 K, these steps are strongly noise-rounded and so we find they are neither visible experimentally at 40 K [6], nor in the simulation in Fig. 4(a) at 20 K.

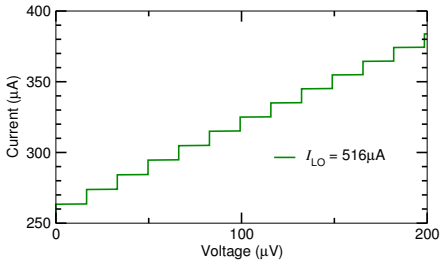

Fig. 6. Part of a simulated I-V curve for $I_c = 774\,\mu$A at $T = 0$ K, with $f_{LO} = 8$ GHz.

For the simulations described below in Sections VI and VII we ran some trials at $T = 0, 20$ and 40 K. The results for all were broadly the same and the difference between the 20 K and 40 K results was not significant. Because simulations at 20 K are faster than those at 40 K, for the same signal-to-noise ratio, we ran some at 20 K, but unless shown otherwise, all results here are at $T = 40$ K.

VI. Dependence on RF and LO amplitudes

We have looked at the variations of IF output and conversion efficiency with DC bias current I_b, for a very wide range of LO and RF currents I_{LO} and I_{RF}. Some representative results are shown in Figs. 7(a) and (b). It shows that η can be as high as -1 dB, which is in line with experimental measurements of -1 dB at 20 K and -3.6 dB at 40 K [6], both of which take into account filter losses and input and output coupling losses in the real MMIC.

A notable feature is a minimum in IF output at a certain value of I_b; this is also seen in experiments, as in Fig. 7(c). We [6] and others [20] have previously attributed this to a point of inflection in the I-V curve. We would expect this to be at the bias current where R_d is a maximum. The simulation results in Fig. 8 show that there is indeed a single maximum in R_d, and like the location of the V_{IF} minimum, it moves to higher I_b with increasing I_{LO}, however, it appears that the minimum in V_{IF} does not quite coincide with the maximum in our estimate of R_d. This issue needs further consideration.

VII. Linearity

The procedure of Section III was adapted to study the linearity of the MMIC, by varying I_{RF} for a range of values of I_{LO}. Simulated dependencies on I_{RF} of the IF output V_{IF} and the conversion efficiency η are shown in Figs. 9(a) and (b), for $I_b = 700\,\mu$A.

We see that η is constant and the output varies linearly with input, up to the point where $I_{RF} \approx I_{LO}$. Beyond that, there is a linear fall in output, followed by a rapid collapse in the output at high values of I_{RF}. Broadly similar features are seen experimentally, as in Fig. 9(c), which shows the behaviour for just one value of P_{LO} [6].

VIII. Conclusions

1. We believe our simulation method is effective, economical and fast, with results which agree well with experiment.
2. In this ideal model, the best conversion efficiency seen was -1 dB for optimum values of $I_b \approx 500\,\mu$A and $I_{LO} = 200\,\mu$A. The optimum operating range is with I_b well below I_c, which is always well clear of the point of zero IF output.
3. We find the same dependence of critical current suppression on LO amplitude as we see in experiments. The dependence is linear, and for $I_{LO} > I_c(0)$, $I_c(I_{LO}) = 0$.

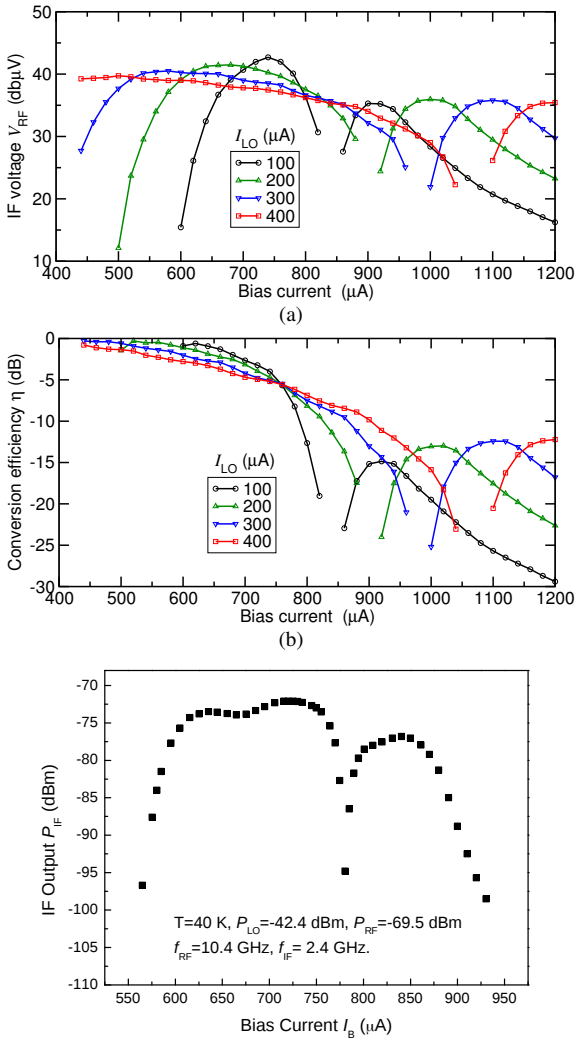

Fig. 7. (a) Simulated IF power and (b) simulated conversion efficiency, as functions of bias current I_b, at $T = 40$ K, for $I_{RF} = 80\,\mu$A. Discontinuities in the data occur where the IF output falls below the noise level and an accurate measure of it cannot be made. (c) Experimental IF power dependence on I_b, also showing a sharp minimum, taken from [6].

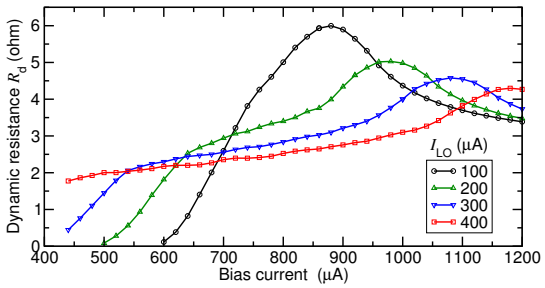

Fig. 8. Estimated dynamic resistance R_d, from simulation at $T = 40$ K, for $I_{RF} = 80\,\mu$A.

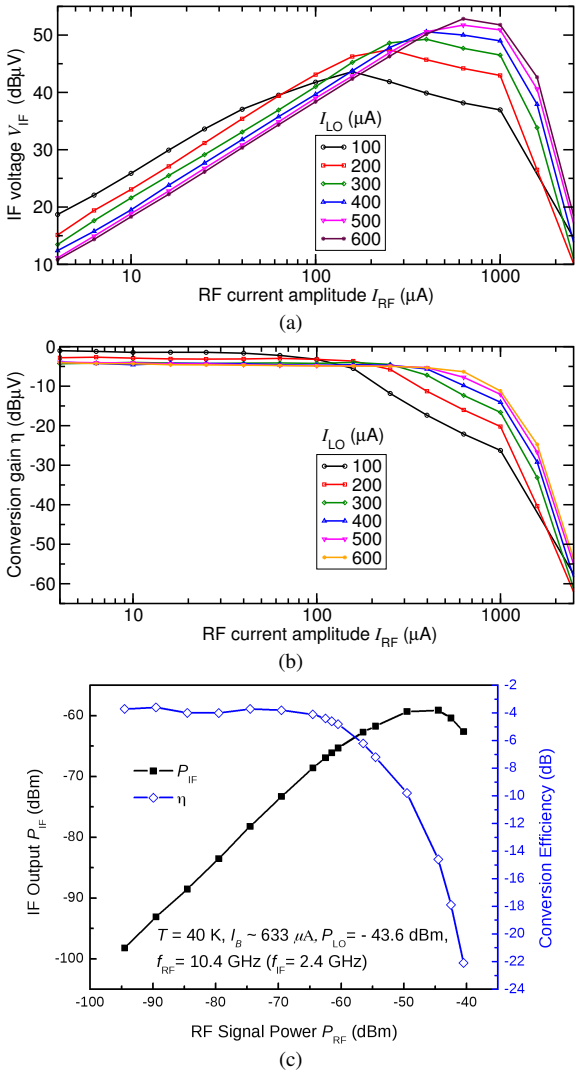

Fig. 9. (a) Simulated IF output voltage amplitude as a function of RF current amplitude, for a range of values of I_{LO}, (b) A similar plot for simulated conversion efficiency η. (c) Experimental data for P_{IF} and η, as a function of RF power P_{RF}, taken from [6].

4. Best linearity is obtained with high LO drive, but the best conversion efficiency is with low LO drive.
5. The minimum in IF output at a certain value of I_{b}, seen in both experiments and simulations, needs further study; it is not clear why other mixing products do not disappear at this same bias point.

ACKNOWLEDGMENT

We thank our collaborators Dr D. D. Bai and Prof Y. S. He of the Institute of Applied Physics, Chinese Academy of Sciences, for their earlier contributions to the experimental results presented in [6].

REFERENCES

[1] C. Foley, E. Mitchell, S. Lam, B. Sankrithyan, Y. Wilson, D. Tilbrook, and S. Morris, "Fabrication and characterisation of YBCO single grain boundary step edge junctions," *IEEE Trans. Appl. Supercond.*, vol. 9, no. 2, pp. 4281–4284, Jun. 1999. [Online]. Available: http://dx.doi.org/10.1109/77.783971

[2] E. E. Mitchell and C. P. Foley, "YBCO step-edge junctions with high $I_{\mathrm{c}}R_{\mathrm{n}}$," *Supercond. Sci. Technol.*, vol. 23, no. 6, p. 065007, Jun. 2010. [Online]. Available: http://dx.doi.org/10.1088/0953-2048/23/6/065007

[3] T. Zhang, J. Du, Y. Guo, and X. W. Sun, "On-chip integration of HTS bandpass and lowpass filters with Josephson mixer," *Electron. Lett.*, vol. 48, no. 12, pp. 729–731, 2012. [Online]. Available: http://dx.doi.org/10.1049/el.2012.1411

[4] T. Zhang, J. Du, Y. J. Guo, and X. Sun, "Design and integration of HTS filters with a Josephson device," *Supercond. Sci. Technol.*, vol. 25, no. 10, p. 105014, 2012. [Online]. Available: http://dx.doi.org/10.1088/0953-2048/25/10/105014

[5] D. D. Bai, J. Du, T. Zhang, and Y. S. He, "A compact high temperature superconducting bandpass filter for integration with a Josephson mixer," *J. Appl. Phys.*, vol. 114, no. 13, p. 133906, 2013. [Online]. Available: http://dx.doi.org/10.1063/1.4824489

[6] J. Du, D. D. Bai, T. Zhang, Y. J. Guo, Y. S. He, and C. M. Pegrum, "Optimised conversion efficiency of a HTS MMIC Josephson down-converter," *Supercond. Sci. Technol.*, vol. 27, no. 10, p. 105002, 2014. [Online]. Available: http://dx.doi.org/10.1088/0953-2048/27/10/105002

[7] J. Du, T. Zhang, Y. J. Guo, and X. W. Sun, "A high-temperature superconducting monolithic microwave integrated Josephson down-converter with high conversion efficiency," *Appl. Phys. Lett.*, vol. 102, no. 21, p. 212602, 2013. [Online]. Available: http://dx.doi.org/10.1063/1.4808106

[8] T. Zhang, J. Du, Y. Guo, and X. Sun, "A $7-8.5$ GHz high performance MMIC HTS Josephson mixer," *IEEE Microw. Wireless Compon. Lett.*, vol. 23, no. 8, pp. 427–429, Aug. 2013. [Online]. Available: http://dx.doi.org/10.1109/LMWC.2013.2269042

[9] T. Zhang, J. Du, J. Wang, D. Bai, Y. Guo, and Y. He, "30 GHz HTS receiver front-end based on monolithic Josephson mixer," *IEEE Trans. Appl, Supercond.*, vol. 25, no. 3, p. 1400605, Jun. 2015. [Online]. Available: http://dx.doi.org/10.1109/TASC.2014.2379095

[10] Advanced Design System (ADS), Keysight Technologies, http://www.keysight.com/en/pc-1297113/advanced-design-system-ads.

[11] E. S. Fang and T. Van Duzer, "A Josephson integrated circuit simulator (JSIM) for superconductive electronics application," in *Extended abstracts, Int. Supercond. Electron. Conf. (ISEC'89), Tokyo, Japan*, 1989, pp. 407–410.

[12] J. Satchell, "Stochastic simulation of SFQ logic," *IEEE Trans. Appl. Supercond.*, vol. 2, no. 7, pp. 3315–3318, Jun. 1997. [Online]. Available: http://dx.doi.org/10.1109/77.622070

[13] Accellera Systems Initiative, http://accellera.org.

[14] T. Zhang, C. Pegrum, J. Du, and Y. J. Guo, "Modeling and simulation of an HTS MMIC Josephson junction mixer," in *Extended abstracts, Int. Supercond. Electron. Conf, (ISEC'15), Nagoya, Japan*, 2015, paper HF-O06.

[15] Quite Universal Circuit Simulator (QUCS), v. 0.0.18, http://qucs.sourceforge.net.

[16] H. Töpfer, G. Mäder, and H. Uhlmann, "Accurate calculation of capacitances of grain boundary Josephson junctions in high critical temperature superconductors," *J. Appl. Phys.*, vol. 77, no. 9, pp. 4576–4579, May 1995. [Online]. Available: http://dx.doi.org/10.1063/1.359421

[17] H. Schmid, "How to use the FFT and Matlab's pwelch function for signal and noise simulations and measurements," Aug. 2012, http://www.fhnw.ch/technik/ime/publikationen/2012.

[18] J. Du, J. C. Macfarlane, C. M. Pegrum, T. Zhang, Y. Cai, and Y. J. Guo, "A self-pumped high-temperature superconducting Josephson mixer: Modelling and measurement," *J. Appl. Phys.*, vol. 111, no. 5, p. 053910, 2012. [Online]. Available: http://dx.doi.org/10.1063/1.3691191

[19] Y. Taur, J. Claassen, and P. Richards, "Josephson junctions as heterodyne detectors," *IEEE Trans. Microw. Theory Techn.*, vol. 22, no. 12, pp. 1005–1009, 1974. [Online]. Available: http://dx.doi.org/10.1109/TMTT.1974.1128414

[20] K. Yamaguchi, A. Kawaji, K. Suzuki, Y. Enomoto, and S. Tanaka, "IF output characteristics of Josephson mixer," *Electron. Comm. Jpn. 2*, vol. 80, no. 3, pp. 69–79, 1997. [Online]. Available: http://dx.doi.org/10.1002/(SICI)1520-6432(199703)80:3⟨69::AID-ECJB8⟩3.0.CO;2-2